Science Translational Medicine
AAAS

www.sciencetranslationalmedicine.org/cgi/content/full/9/388/eaad9157/DC1

Supplementary Materials for

Mutations in the vesicular trafficking protein annexin A11 are associated with amyotrophic lateral sclerosis

Bradley N. Smith, Simon D. Topp, Claudia Fallini, Hideki Shibata, Han-Jou Chen, Claire Troakes, Andrew King, Nicola Ticozzi, Kevin P. Kenna, Athina Soragia-Gkazi, Jack W. Miller, Akane Sato, Diana Marques Dias, Maryangel Jeon, Caroline Vance, Chun Hao Wong, Martina de Majo, Wejdan Kattuah, Jacqueline C. Mitchell, Emma L. Scotter, Nicholas W. Parkin, Peter C. Sapp, Matthew Nolan, Peter J. Nestor, Michael Simpson, Michael Weale, Monkel Lek, Frank Baas, J. M. Vianney de Jong, Anneloor L. M. A. ten Asbroek, Alberto Garcia Redondo, Jesús Esteban-Pérez, Cinzia Tiloca, Federico Verde, Stefano Duga, Nigel Leigh, Hardev Pall, Karen E. Morrison, Ammar Al-Chalabi, Pamela J. Shaw, Janine Kirby, Martin R. Turner, Kevin Talbot, Orla Hardiman, Jonathan D. Glass, Jacqueline de Belleroche, Masatoshi Maki, Stephen E. Moss, Christopher Miller, Cinzia Gellera, Antonia Ratti, Safa Al-Sarraj, Robert H. Brown Jr., Vincenzo Silani, John E. Landers, Christopher E. Shaw*

*Corresponding author. Email: chris.shaw@kcl.ac.uk

Published 3 May 2017, *Sci. Transl. Med.* **9**, eaad9157 (2017)
DOI: 10.1126/scitranslmed.aad9157

The PDF file includes:

Fig. S1. The *ANXA11* p.D40G mutation shares a common haplotype composed of four exonic SNPs and two microsatellites.
Fig. S2. Haplotype gene map of the *ANXA11* p.D40G locus.
Fig. S3. Annexin A11 Western blot of lysates made from postmortem tissue of the SALS patient harboring the p.D40G mutation and control individuals.
Fig. S4. p.R235Q ANXA11-GFP colocalizes with ubiquitin and p62 in HEK cells.
Fig. S5. Modeling of annexin A11 identifies two amphipathic helices in the N terminus of annexin A11 that overlap with the G38 and D40 residues.
Fig. S6. Twenty-two ExAC polymorphisms spanning the D40 locus do not disrupt the formation of amphipathic helices.
Fig. S7. Rare and common *ANXA11* polymorphisms do not disrupt calcyclin binding compared to ALS-specific variants.

Fig. S8. N-terminal annexin A11 mutations do not alter binding of sorcin and ALG-2.

Other Supplementary Material for this manuscript includes the following:
(available at www.sciencetranslationalmedicine.org/cgi/content/full/9/388/eaad9157/DC1)

Table S1 (Microsoft Excel format). New variants shared between members of each familial ALS family.
Table S2 (Microsoft Excel format). New variants shared between *ANXA11* p.D40G families.
Table S3 (Microsoft Excel format). Homogeneity of the FALS cohort and ExAC NFEs.
Table S4 (Microsoft Excel format). Primer sequences used in the *ANXA11* p.D40G haplotype study and for Sanger sequencing of *ANXA11* exons.
Table S5 (Microsoft Excel format). Exon coverage data of genes within the minimal p.D40G haplotype region.
Table S6 (Microsoft Excel format). All variants found within *ANXA11* in FALS and SALS.
Table S7 (Microsoft Excel format). Clinical details of patients with *ANXA11* mutations.

				Family 1				Family 2											
Marker	Position Hg19 (Chr10)	Gene	Allele Variant	III-2		III-5		III-19		III-18		IV-12		IV-13		II-2		Sporadic	
22xTG	78303074-78303119	NA	$(TG)_n$	272	292	272	290	288	274	274	278	274	274	274	274	274	274	272	290
21xAC	80615142-80615185	NA	$(AC)_n$	315	309	317	309	311	309	315	313	315	309	315	309	309	309	317	309
rs41291392	81904645	PLAC9	C>T	C	T	C	T	C	T	C	C	C	T	C	T	C	T	C	T
ANXA11 A>G	81930608	ANXA11	A>G	A	G	A	G	A	G	A	A	A	G	A	G	A	G	A	G
rs17617713	82191700	FAM213A	G>A	G	A	G	A	G	A	G	G	G	A	G	A	G	A	G	A
rs72821609	82276061	TSPAN14	C>T	C	T	C	T	C	T	C	C	C	T	C	T	C	T	C	T
rs72805713	82331416	SH2D4B	A>G	A	G	A	G	A	G	A	A	A	G	A	G	A	G	A	G
25xAT	83185144-83185195	NA	$(AT)_n$	248	250	248	250	250	250	248	240	248	250	248	250	250	250	272	250
24xAG	85399588-85399637	NA	$(AG)_n$	277	273	265	275	277	273	271	255	271	273	271	273	273	273	277	289
24xAC	87562595-87562642	NA	$(AC)_n$	278	288	276	276	278	278	276	280	276	278	278	280	280	280	278	282

Supplementary Figure 1. The *ANXA11* p.D40G mutation shares a common haplotype composed of four exonic SNPs and two microsatellites. Genotyping of 5 polymorphic microsatellites spanning the *ANXA11* locus identified the 7.1MB maximal recombination region between microsatellites 22xTG and 24xAG (marked in red). The 2.5Mb minimal common region specific to all UK affected ALS p.D40G patients (4 FALS and 1 sporadic ALS case) was defined by two microsatellites (21xAC and 25xAT) and 4 exonic SNPs (rs41291392, rs17617713, rs72821609 and rs72805713), ie. 309-T-G-T-G-250. Genotyping of an unaffected spouse (Generation III-18) and two unaffected p.D40G carriers (Generation IV-12 and IV-13) from Family 2 (Figure 1C) determined haplotype phase.

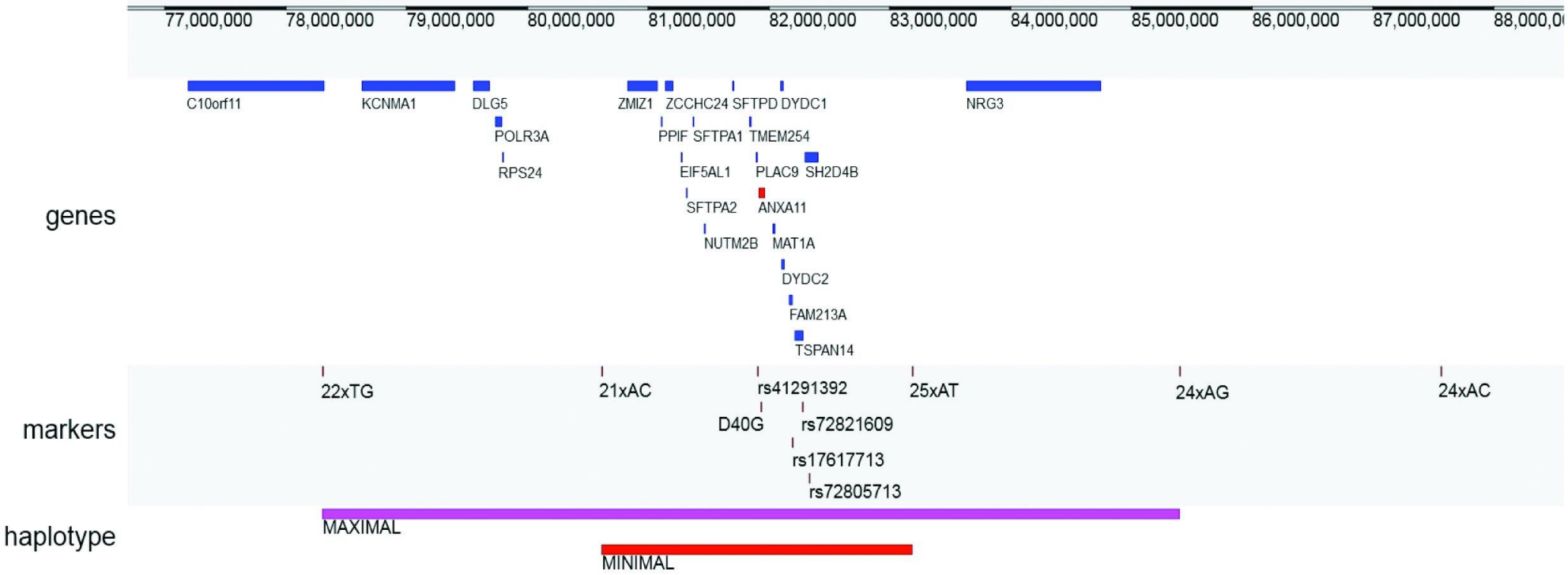

Supplementary Figure 2. Haplotype gene map of the *ANXA11* p.D40G locus. The maximal haplotype region (~7.1MB) is defined by the outer limit of recombination at the two flanking microsatellites 24xAG and 22xTG (pink region). The minimal common p.D40G haplotype block (~2.5MB) spans *ANXA11* and is shared by all 5 affected ALS UK cases and two unaffected ALS carriers. Exome sequencing of p.D40G carriers identified no additional novel or rare exonic or splicing variants in the 23 genes located within this maximal locus.

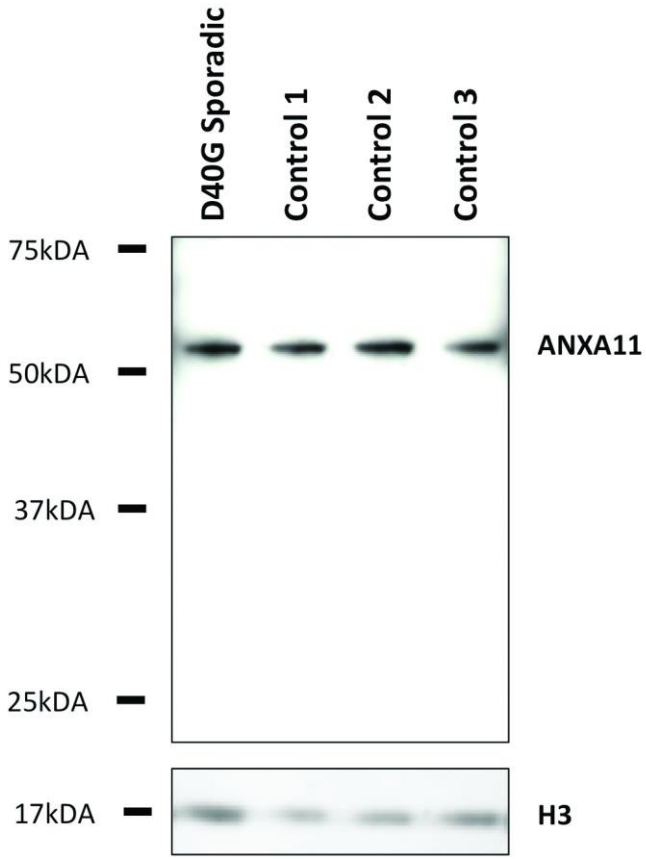

Supplementary Figure 3. Annexin A11 Western blot of lysates made from postmortem tissue of the SALS patient harboring the p.D40G mutation and control individuals. Western blotting of lysates made from frontal cortex tissue of the sporadic patient harbouring the p.D40G mutation, using a polyclonal Rabbit Annexin A11 antibody, yields a specific single band at ~55kDA. There was no difference in Annexin A11 expression due to the p.D40G mutation compared to lysates made from three control individuals.

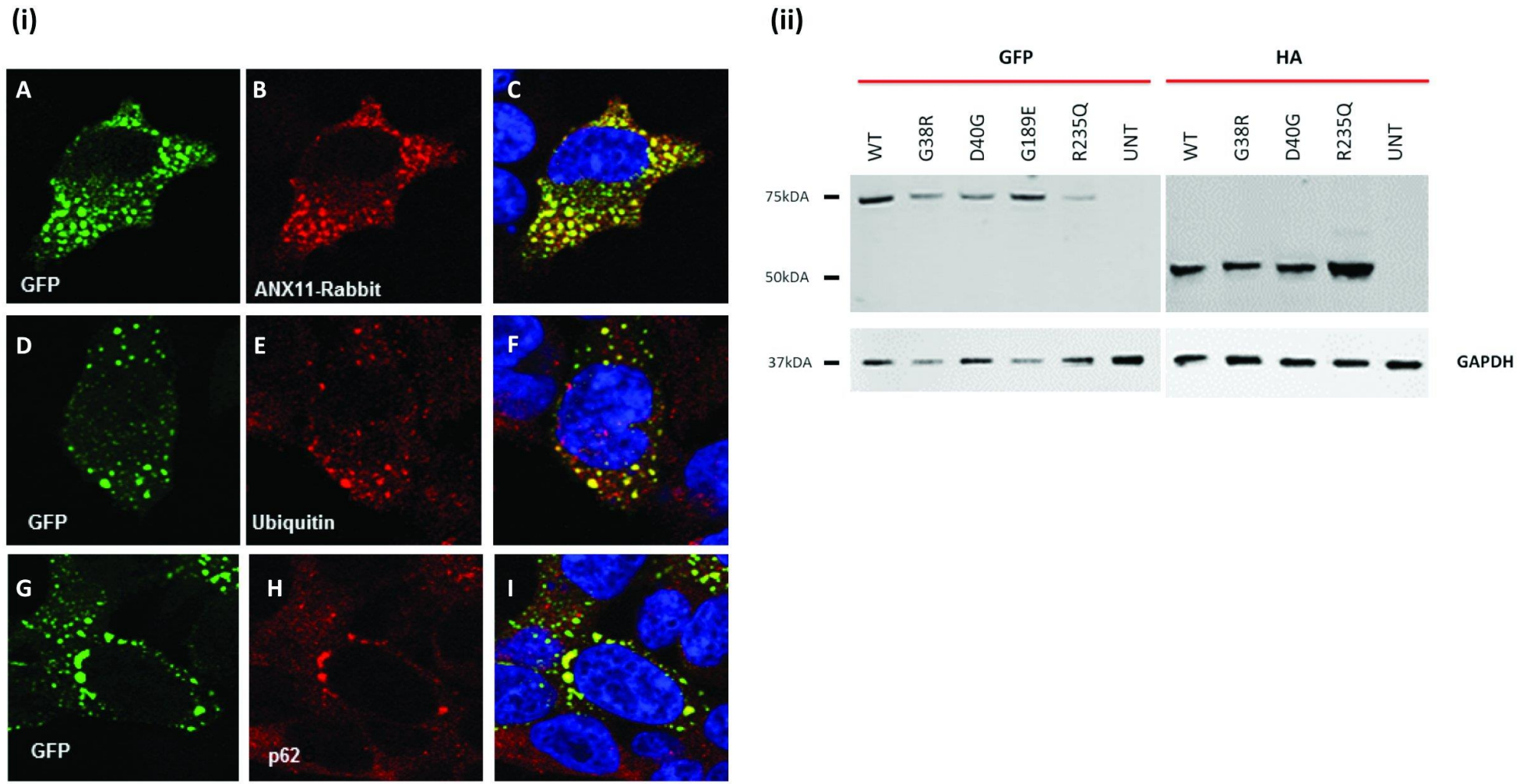

Supplementary Figure 4. p.R235Q ANXA11-GFP colocalises with ubiquitin and p62 in HEK cells. (i) Cells were transfected with ANXA11-GFP^{R235Q} for 48hrs, fixed and stained with the following antibodies by immuno-cytohistochemistry (ICC) (A) mouse GFP - green. (B) ANXA11 Polyclonal rabbit Antibody (Proteintech) - red. (C) Merge of A, B and DAPI blue nuclear staining, showing specificity of ANXA11 specific antibody, (D) mouse GFP - green. (E) Rabbit K-48 Ubiquitin - red. (F) Merge of D, E and DAPI. (G) mGFP - green. (H) Rabbit p62 - red. (I) Merge of G, H and DAPI blue nuclear staining (ii) Confirmation of specificity of endogenous Rabbit ANXA11 antibody in ICC (as used in 4(i) A-C) for GFP and HA tagged ANXA11 constructs by Western blot.

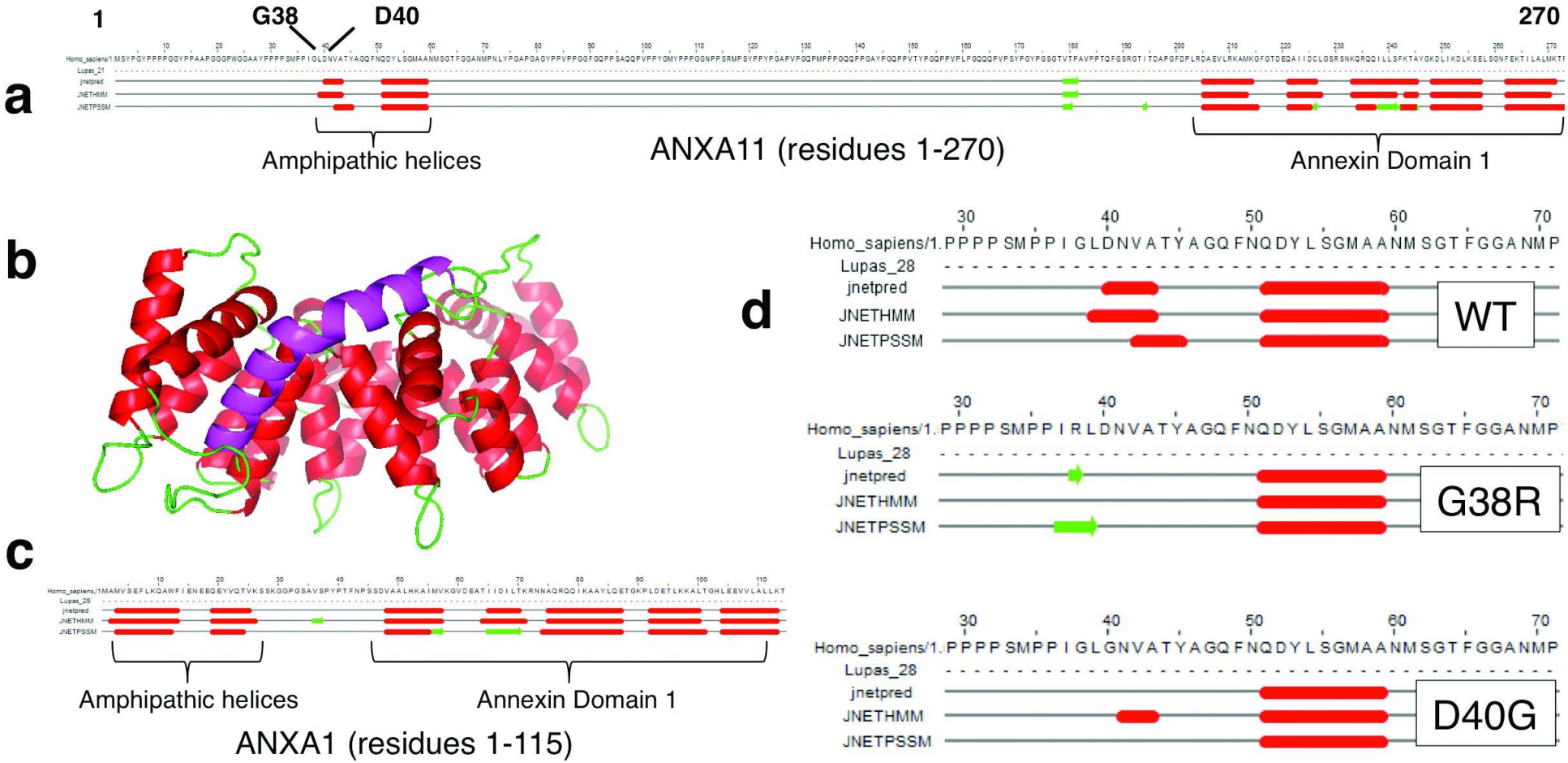

Supplementary Figure 5. Modeling of annexin A11 identifies two amphipathic helices in the N terminus of annexin A11 that overlap the G38 and D40 residues. (A) Jpred secondary structure prediction of the N-terminus (residues 1-270) using a multiple alignment of 30 mammalian orthologue sequences identified two alpha helices, indicated in red (residues 40-44 and 51-59). Green represents potential beta strands. Known annexin domains start at ~205 residues. The locations of the G38 and D40 residues are indicated in the first helix. (B) Protein structure of annexin A1 (pdb:1hm6) in the presence of calcium, with the annexin domain alpha helices in red and the N-terminal helices in magenta. (C) Jpred also predicts the N-terminus of annexin A1 to possess two alpha helices (residues 3-13 and 19-25). (D) The Jnetpred consensus (top row) predicts that both the p.G38R and the p.D40G variants abolish the first alpha helix.

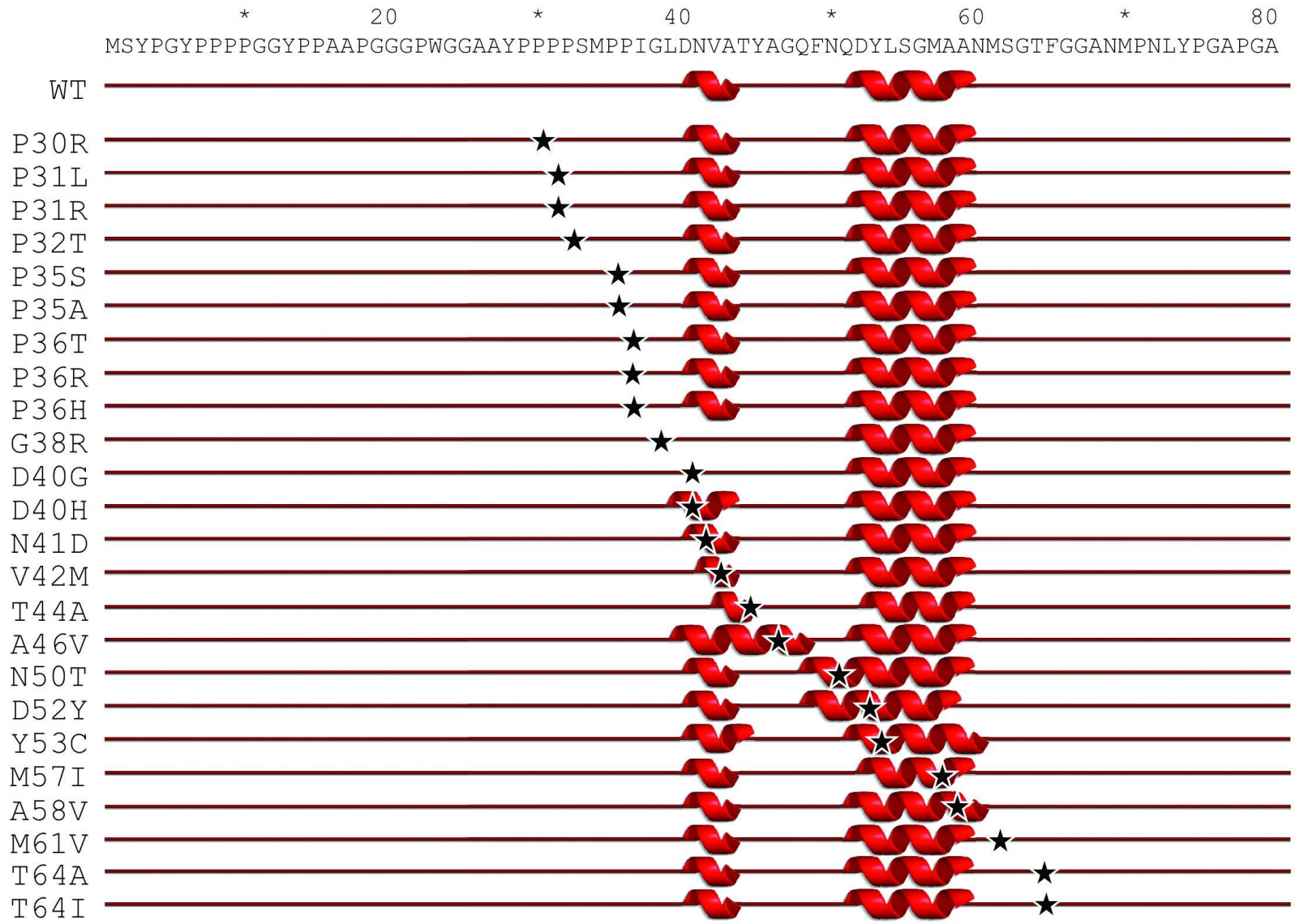

Supplementary Figure 6. Twenty-two ExAC polymorphisms spanning the D40 locus do not disrupt the formation of amphipathic helices. Secondary structure predictions on the N-terminus of Annexin 11 show that only the ALS-linked mutations p.G38R and p.D40G completely abolish the formation of the first alpha helix. None of the 22 ExAC variants flanking this region, including p.D40H, have the same effect. Secondary structures were derived from Jpred4 consensus, performed on a multiple alignment of 30 mammalian orthologues.

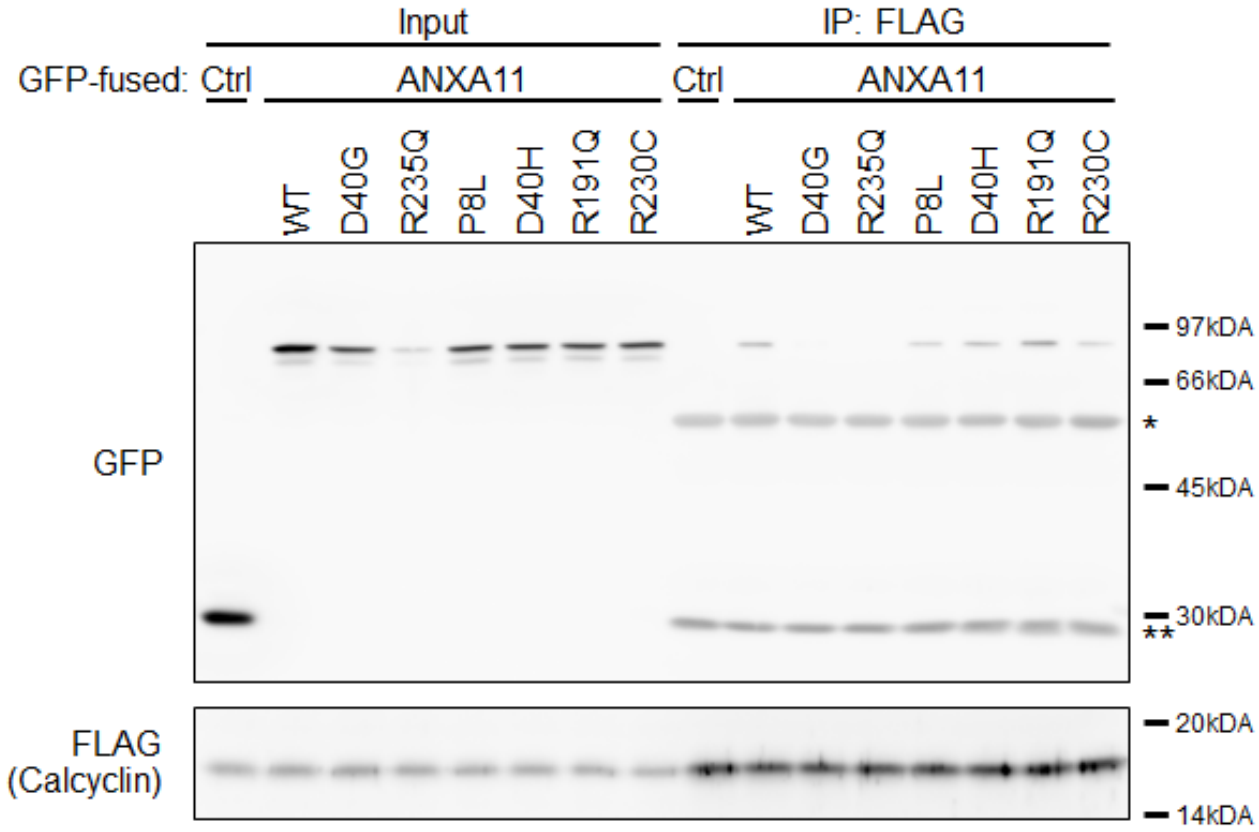

Supplementary Figure 7. Rare and common *ANXA11* polymorphisms do not disrupt calcyclin binding compared to ALS-specific variants. Immunoprecipitation (IP) of FLAG-calcyclin from mixed lysates of HEK cells expressing GFP-fused proteins (as indicated) in the presence of calcium show similar binding affinities for the p.P8L, the p.D40H, the p.R191Q and the p.R230C to that of wild-type (WT) when probed for GFP (n=3). The top panel shows GFP intensities of input and pulldown fractions, with IgG heavy (*) and light chains (**) indicated. The bottom panel illustrates input and IP levels of FLAG-calcyclin.

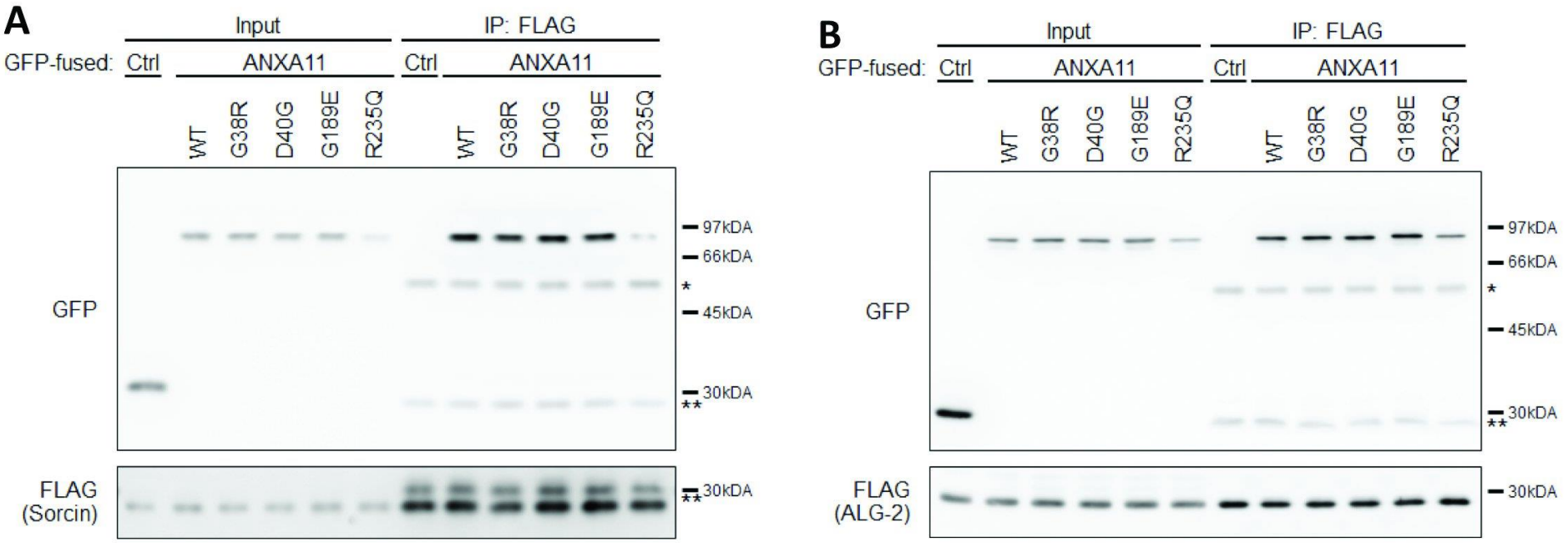

Supplementary Figure 8. N-terminal annexin A11 mutations do not alter binding of sorcin and ALG-2. (A) Immunoprecipitation (IP) of FLAG-Sorcin from mixed lysates of HEK cells transfected with ANXA11-GFP$^{WT+G38R+D40G+G189E+R235Q}$ activated with calcium show no difference in binding between ANXA11 WT and mutants when probed for GFP. (B) The same was seen when IP was conducted with ALG-2 and sorcin. (n=3). The top panel shows GFP intensities of input and pulldown fractions, with IgG heavy and light chains indicated. The bottom panel for both (A) and (B) illustrates input and IP levels of FLAG-sorcin or FLAG-ALG-2 respectively.